3-D Direction of Arrival Estimation with Two Antennas

Xiaoju Yu [(1)], Hao Xin* [(1)]
(1) Electrical and Computer Engineering Department,
University of Arizona, Tucson, AZ 85721

ABSTRACT

Inspired by human auditory system, an improved direction of arrival (DOA) technique using only two antennas with a scatterer in between them to achieve additional magnitude cues is proposed. By exploiting the incident-angle-dependent magnitude and phase differences between the two monopole antennas and applying 2-D / 3-D multiple signal classification algorithms (MUSIC), the DOA of an incident microwave signal can be estimated. Genetic algorithm is applied to optimize the scatterer geometry for the 3-D DOA estimation. The simulated results of both the azimuth and three-dimensional DOA estimation have shown an encouraging accuracy and sensitivity by incorporating a lossy scatterer.

Key Words: 3-D Direction of Arrival, Biological Inspired, Scatterer, Magnitude and Phase Difference

INTRODUCTION

Direction of arrival (DOA) estimation of an electromagnetic signal is important for many commercial and military applications including electronic warfare [1], mobile communications [2]. Most attention has been paid on arrays consisting of a large number of antennas and sophisticated algorithms to achieve high degree of accuracy [1]. However, as the number of antenna elements increases, the power consumption, size and cost of the system increase as well, which would be impractical especially for portable and commercial applications. Therefore, accurate DOA estimation technique with reduced number of antennas is highly desirable.

Passive direction finding for microwave signal is very analogous to the direction finding of acoustic wave by human ears. Figure 1 illustrates the analogy between a microwave direction finding system and the human auditory system. The microwave antennas are similar to the pinnae, which are natural directional antennas for acoustic waves; the band-pass filters, amplifiers, mixers and detectors provide similar functions as the guiding and detecting parts of the human auditory system; and the signal processing component can be thought as the brain.

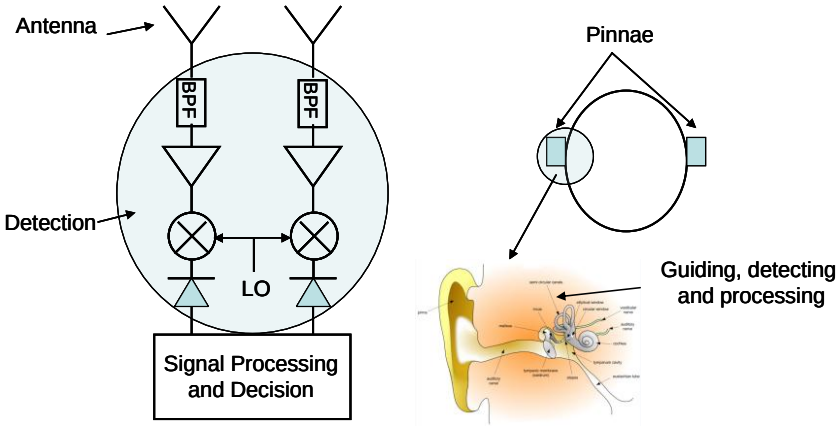

Figure 1. Comparison of a passive microwave direction finding system (left) and the human auditory system (right).

The remarkable localization (mainly in the azimuth plane) capabilities of human ears for both continuous waves (CW) and transient signals have long been recognized and studied quite extensively [3-8]. Many intriguing facts and phenomena were experimentally observed and underlying mechanisms were proposed and proved. As early as 1936, Stevens and Newman reported free space experimental data on localization of sound sources by human ears which revealed the two main mechanisms of binaural sound localization, one operating best at high frequency and the other at low frequency [6]. Later on, more studies in anechoic chambers confirmed the earlier results [7-8]. For most of the audible frequency range (20 Hz – 20 KHz), human ears have the amazing ability of estimating arrival angle with accuracy up to 1 ° without ambiguity under binaural (utilizing two ears) conditions.

For low frequency sound (f <1.5 – 3.0 KHz), the phase difference between the acoustic signals received by the two ears (referred to as the binaural case) serves as the most important cue. To avoid the phase ambiguity of multiples of 2π, the antenna elements should be spaced less than half a wavelength, $\lambda/2$. The front-back ambiguity is eliminated by the directivity of human ears (analogous to an antenna radiation pattern) [3]. For higher frequency sound (f > 3.0 KHz), the head can be thought as a low-pass filter. For most incident angles, one ear receives without the influence of the head while the other receives after the incident signal goes through (or around) the low-pass filter - human head, whose response function is incident angle dependent and can have an attenuation as much as 20 dB [5]. This effect is often referred to as the head-related-transfer function (HRTF), which leads to both a phase and a magnitude difference between the received signals at two ears. The combination of the phase (or time for transient signals) and amplitude information enables the human auditory system to have great localization capabilities for both low and high frequency ranges.

Both of the binaural mechanisms mentioned above have analogies or may be directly applied to microwave systems. The low-frequency phase difference method is widely used in microwave direction finding [1]. The high-frequency scheme utilizing an effective low-pass filter (the shadowing effect of human head) for azimuth-plane direction finding has been reported in [9][10]. By introducing a carefully designed scatterer in between two adjacent antennas, accurate direction finding without phase ambiguity for high frequency signals may be achieved. Furthermore, because of the spacing between the adjacent antenna elements can now be much

larger than λ/2, the mutual coupling issue that is common to antenna array systems can be greatly reduced. In this paper, more comprehensive and improved design for 2-D direction finding is described. In addition, 3-D (azimuth and elevation) direction finding technique is proposed by optimizing the scatter geometry and material parameters.

2-D DIRECTION FINDING

To evaluate the feasibility of applying some of the human sound localization mechanisms in microwave direction finding, a simple two-antenna (omni-directional monopoles are used here for simplicity) configuration is considered. Take an electromagnetic (EM) signal coming from an azimuth direction θ that is impinging on two monopole antennas separated by a distance d, as shown in Figure 2, the phase difference ΔΨ between the received signals at these two antennas is, $\Delta\Psi = \frac{d\sin\theta}{\lambda}2\pi$, where λ is the wavelength of the signal. It can be derived that for both EM and acoustic DOA, if d is greater than half wavelength, there may be ambiguities in the estimated DOA. To avoid this kind of ambiguity at high frequency, it is proposed here that a lossy scatterer is placed between the two antennas, providing the similar low-pass filtering function as the human head between two ears. Without the scatterer, the phase difference ΔΨ of the signals measured at the two antennas is the key information to estimate the DOA. With the scatterer, the magnitude difference ΔM provides an additional important cue in the DOA estimation, eliminating the phase ambiguity issue.

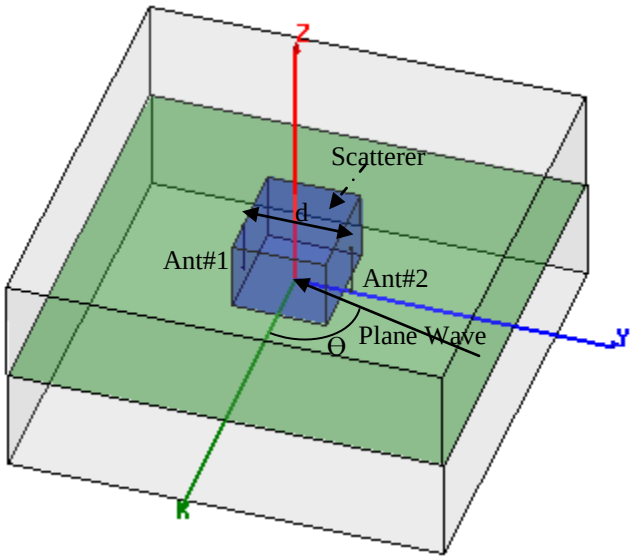

Figure 2. A finite-element model illustrating the geometry of the two-monopole/scatterer configuration with an incoming signal from an azimuth angle.

To evaluate the DOA performance of the two-monopole / scatter system, phase differences ΔΨ and magnitude differences ΔM between the two monopoles as a function of incident angle from $0°$ to $360°$ are first simulated in full-wave finite-element EM solver High-Frequency-Structure-Simulator (HFSS) and saved as the calibration steering vectors. Then, for an arbitrary incident

angle θ, assuming a phase error (2˚) and magnitude error (0.25dB), the multiple signal classification (MUSIC) algorithm [11] is used to estimate the DOA. The simple configuration in Figure 2 (with / out a lossy scatterer) works at X-band (8 – 12 GHz) with monopole length 7 mm and monopoles spacing d 15 mm (λ/2 at center frequency 10 GHz). The scatterer used here is a lossy material, ARC-LS-10211 (made by ARC Technologies Inc.), with ε = 2.05 and tanδ = 1.15 and dimensions of 15 mm x 12.8 mm x 10 mm.

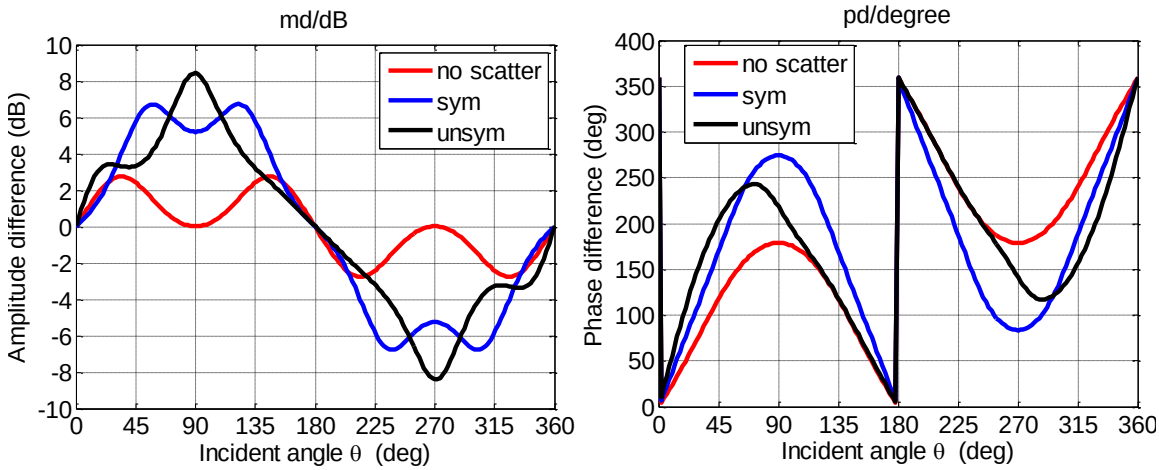

Figure 3. simulated magnitude (left) and phase (right) differences at 10 GHz for the three cases: No scatterer (red line); Symmetric scatterer (blue line); Un-symmetric scatterer (black line).

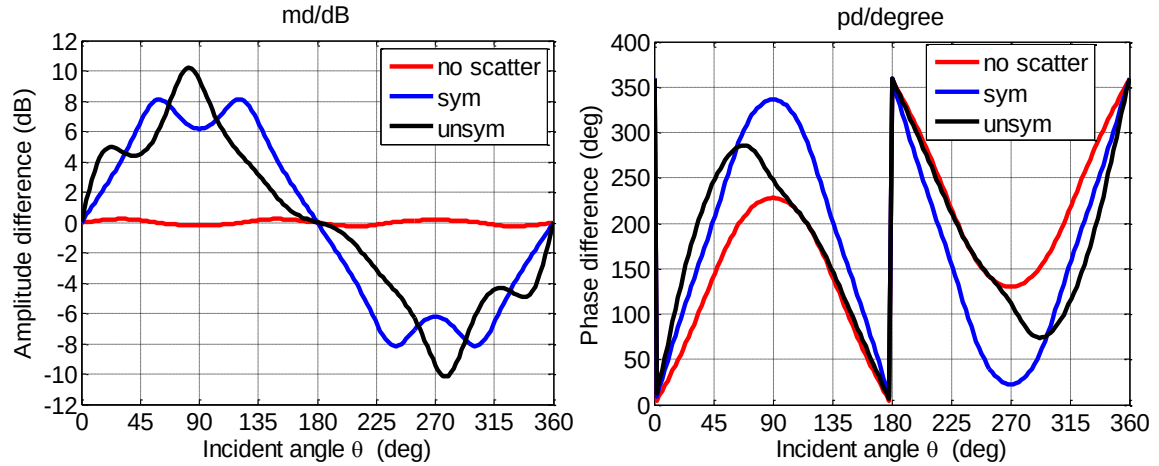

Figure 4. simulated magnitude (left) and phase (right) differences at 12 GHz for the three cases: No scatterer (red line); Symmetric scatterer (blue line); Un-symmetric scatterer (black line).

Figures 3-4 plot the simulated ΔΨ and ΔM at 10 and 12 GHz, without the lossy scatterer, with symmetric and asymmetric scatterer. It can be pointed out that with the lossy scatterer, the magnitude difference is much larger as expected. In addition, the phase difference versus incident angle curve with the scatterer is significantly steeper than that without the scatterer, which indicates increased sensitivity in the DOA estimation. Although the phase ambiguity issue seems to be more severe for the case with the scatterer, the large magnitude differences will be sufficient to overcome the ambiguities. However, both the phase and magnitude differences

without the scatterer and with symmetric scatterer are the same for supplementary incident angles (e.g., front / back ambiguity), which is due to the symmetry respect to the y-axis (refer to Figure 2). This can be solved by either using directional antennas just as the human ears or breaking the symmetry of the scatterer. By shifting the two monopoles toward one side of the scatterer block by 7.5 mm, the case with asymmetric scatterer is also represented in Figures 3-4. The results with asymmetric scatterer show a promising improvement against the front-back ambiguity.

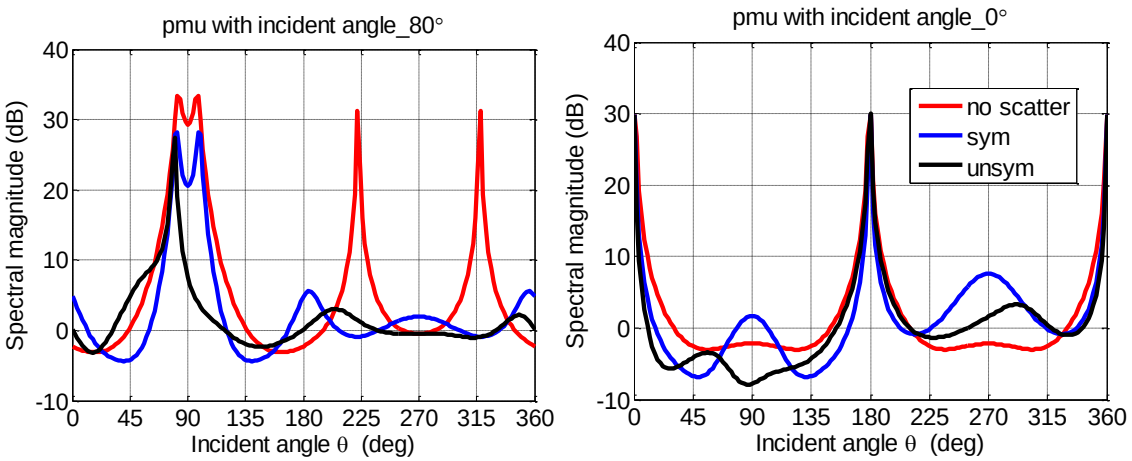

Figure 5. Simulated MUSIC output of the three scenarios with a 12GHz signal incident from the 80 ° direction (left figure) and the 0 ° direction (right figure): without a scatterer (red line), with a symmetrically positioned rectangular scatterer (blue line) and with an asymmetrically positioned rectangular scatterer (black).

In Figure 5, the MUSIC output for the simulated case with a 12 GHz signal coming from the 80 ° and 0 ° direction is plotted for the three scenarios mentioned above (without scatterer, symmetric scatterer and asymmetric scatterer). It is clear that the addition of the attenuating scatterer (similar to the low-pass-filter function of the human head) in between the two antennas eliminates the ambiguity caused by the 2π phase wrapping. Moreover, it can be observed from Figure 5 that the asymmetrically placed scatterer breaks the front / back symmetry and eliminates the corresponding ambiguity at some angle as well. For the no scatterer case at incident angle of 80 °, there are four peaks near 80 ° (100 °) and 222 ° (319 °) that can be observed, for which the 80 ° and 222 ° ambiguity is due to the greater than $\lambda/2$ spacing of the monopoles. With the scatterer, this ambiguity is clearly eliminated by the added magnitude information, which can be seen from both the symmetric and asymmetric cases in Figure 5. The 80 ° and 100 ° ambiguity manifested in the no scatterer and symmetric scatterer cases is due to the front / back symmetry of the two-antenna system, which is absent in the asymmetric configuration. When the incident angle is 0 °, however, there are two peaks near 0 ° and 180 ° for both without and with scatterer case. Figure 4 shows that both the magnitude difference and phase difference are zero at 0 ° and 180 ° without / with scatterer. In order to eliminate this ambiguity, the symmetry respect to x axis has to be broken. Thus a new configuration named “scatter3” is offered in Figure 6 with Block#1 of ε = 2.05, tanδ = 1.15 and dimensions of 15 mm x 10 mm x 10 mm and Block#2 of ε = 2.05, tanδ = 20 and dimensions of 15 mm x 2.8 mm x 10 mm.

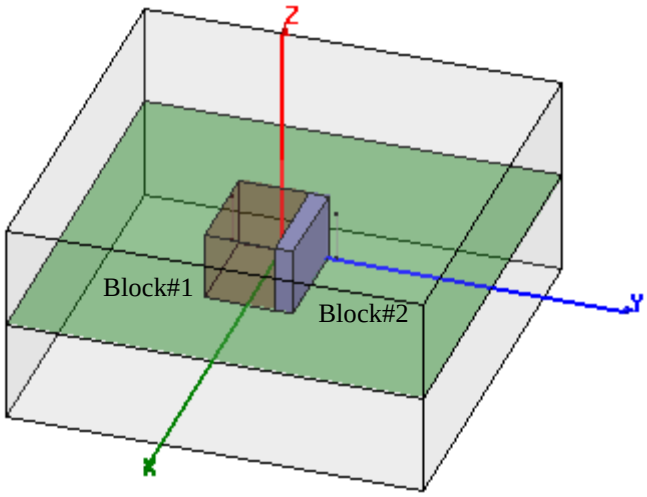

Figure 6. Schematic of scatter3.

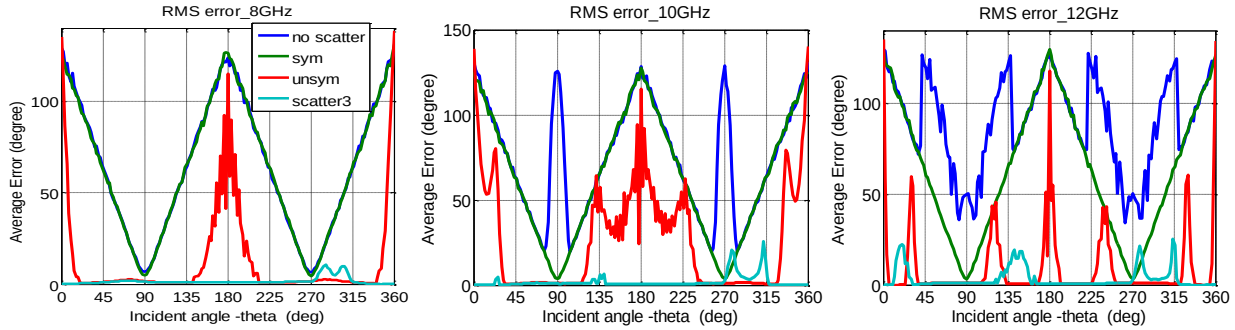

Figure 7. Root mean square of DOA estimation errors of the incident signal at 8GHz (left), 10GHz (middle) and 12GHz (right) for 4 cases: no scatterer (blue), symmetric scatterer (green), asymmetric scatterer (red) and scatter3 (light blue).

Figure 7 shows the root mean square of DOA estimation errors with a Gaussian distributed phase difference error (μ=0, σ=2˚) and magnitude difference error (μ=0, σ=0.25dB) of the incident signal at 8GHz, 10GHz and 12GHz for 4 cases: no scatterer, symmetric scatterer, asymmetric scatterer and scatter3. The angle where the maximum output of MUSIC algorithm occurs is assumed to be the true incident angle. With no scatterer, the RMS error is large with maximum error about 140˚ at 0˚ and 180˚. With symmetric scatterer, the RMS error is reduced at some angle. With asymmetric scatterer, the RMS error is further decreased but still high at 0˚ and 180˚. When scatter3 is applied, the 0˚ and 180˚ ambiguity is eliminated and the RMS error is low at all angles. The RMS error is lower than 2˚ at most of the incident directions and the maximum error is about 25˚. Thus a two-monopoles/scatterer configuration with good DOA estimation accuracy is achieved.

3-D DIRECTION FINDING

The essence of this direction finding technique is to get the incident angle dependent combination of phase and amplitude information. From the previous 2-D direction finding

analysis, it is obvious that the scatterer geometry and material parameters matter much in the DOA estimation accuracy. If the scatter is optimized such that the receiving response function is incident angle dependent for all directions including azimuth and elevation, this technique may be extended to achieve three-dimensional direction finding (DF). In the following we explore genetic algorithm to optimize the scatterer with the goal of achieving 3-D DF.

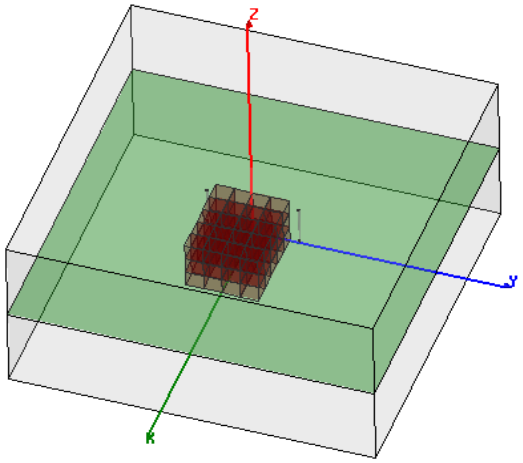

Figure 8. Original geometry of the monopole/scatterer system.

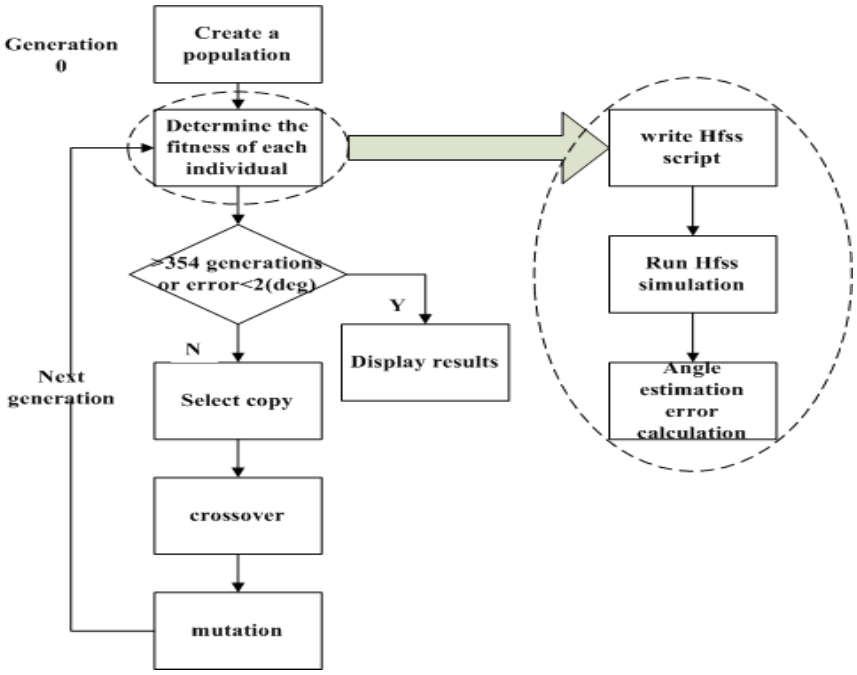

Figure 9. Genetic optimization procedure.

As shown in Figure 8, the original asymmetric scatterer is divided into 5×4×3=60 blocks with every block of $3mm^3$ ($\varepsilon = 2.05$ and $\tan\delta = 1.15$). "1" represents the lossy block exists and "0" means a substitute of air in place of the lossy block. Thus every sequence of 60 binary digits represents one kind of scatterer geometry. Genetic algorithm [12] is applied to optimize the scatterer geometry. Figure 9 illustrates the procedure of this optimization. The population size is

4 (4 simulations each time). The goal is set to obtain the average error of the estimated DOA smaller than 2°. First a population with 4 individuals (each carry a sequence of 60 binary digits) is generated and according to this, a HFSS script is written to set up the geometry models. After the HFSS models are generated, these models would be simulated and the magnitude and phase information received at the two monopoles would be saved. Then this information would be used to calculate the DOA estimation error in matlab software. Finally a decision would be made that if the goal is achieved, the procedure should stop, if not, a new generation would be generated. To evaluate the DOA performance of the two- λ/4 monopole / scatterer system, the simulated phase and magnitude differences of the received signals between the two monopoles as a function of incident angle (θ, ϕ) are saved as the calibration steering vectors (θ is 10°~ 90°and ϕ is 0°~ 350°with 10°step). Then, for an arbitrary incident angle (θ, ϕ) assuming a phase error (+/- 2°) and a magnitude error (+/- 0.25dB), the 3-D multiple signal classification (MUSIC) algorithm is used to estimate the DOA. In order to better evaluate the system we propose the average error: $\sum_{ij} \frac{\sqrt{\Delta\theta_i^2 + \Delta\phi_j^2}}{MN}$ as the assessment criteria, where M is the total number of ϕ and N is the total number of θ.

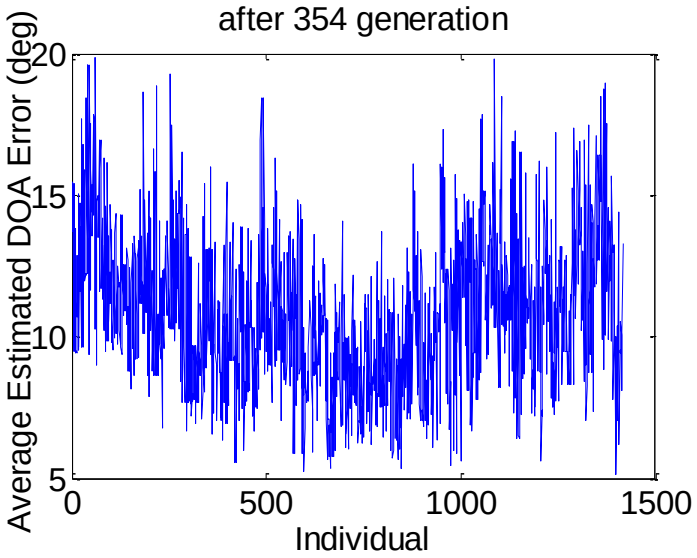

Figure 10. Genetic optimization results after 354 generation with total 354×4=1416 geometries.

Figure 10 is the optimization result after 354 generation at 12GHz. It takes about 3 weeks to finish this optimization (i7 CPU, 2.67GHz with 12GB memory). The smallest average error is about 5°. Figure 11 shows the schematic of the best case. With this configuration, we simulated the received magnitude and phase differences but with finer angle sweeping where the incident angle θ is 2°~ 90°and ϕ is 0°~ 358°with 2°step. From comparison between the estimated DOAs and the original true incident angles we can plot the estimated error of θ and ϕ as a function of the incident angle (θ, ϕ) as shown in Figure 12. There are large errors at ϕ=0°and 180°where the magnitude and phase differences are nearly 0. Errors are also large when θ is near 0°where the arc lengths are shortest. Nevertheless, most of the incident angles have quite small error, demonstrating a promising technique for estimation of DOA from all directions in three-dimensional space.

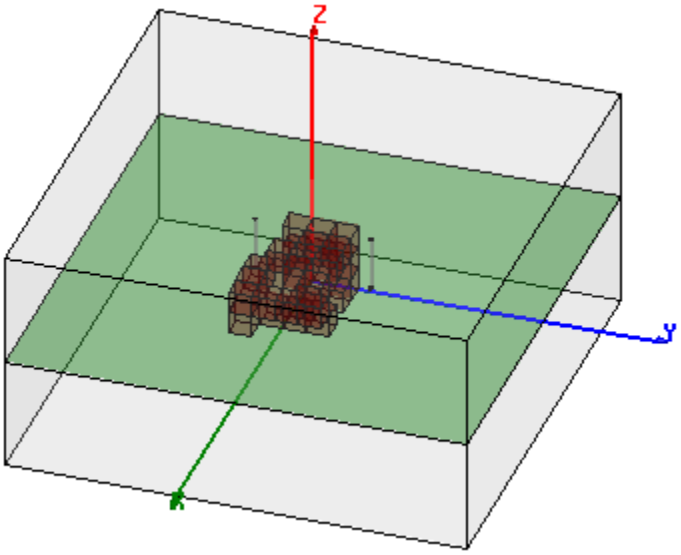

Figure 11. The geometry of th
e best case of the optimization.

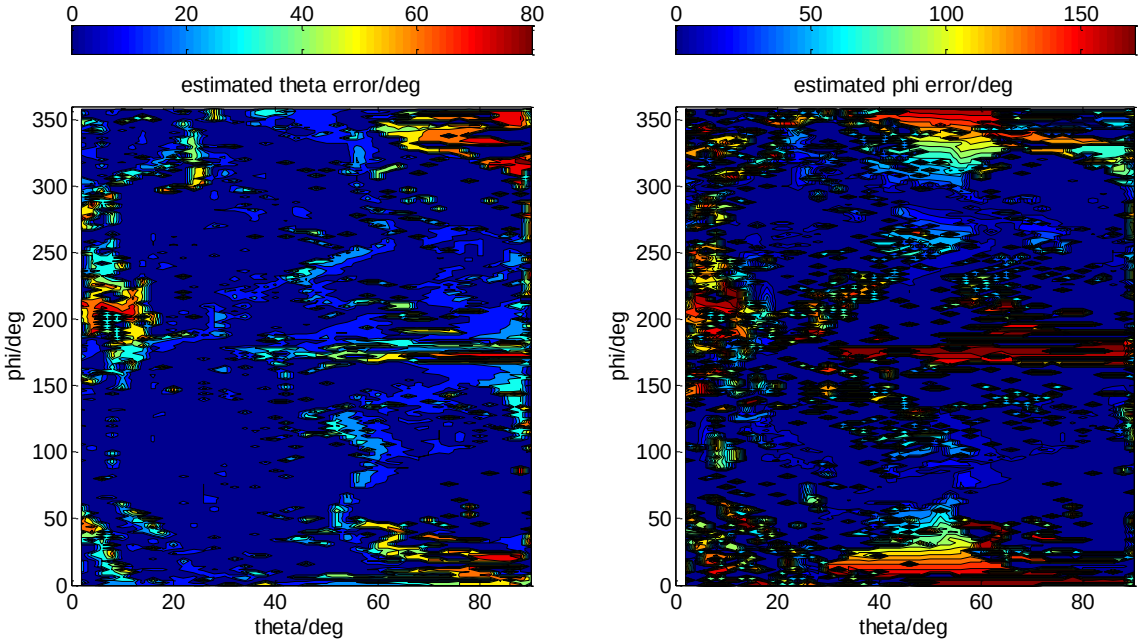

Figure 12. Estimated θ error (left figure) and ϕ error (right figure) of the best case. The x axis is the true incident θ and y axis the true incident ϕ.

CONCLUSION

Human ears have the amazing ability of estimating arrival angle (mainly in the azimuth plane) with accuracy up to 1 °without ambiguity under binaural (utilizing two ears) conditions. Inspired by the human auditory system, an improved DOA technique using only two antennas with a scatter in between them, emulating the low-pass filtering function of the human head at high frequency to achieve additional magnitude cues, has been described. By exploiting the incident-angle-dependent magnitude and phase differences between the two monopole antennas and 2-D/ 3-D multiple signal classification algorithm (MUSIC), the DOA of a microwave signal can be estimated. A simple 2-monopole example at X-band frequency (8 to 12 GHz) is studied. Simulated results of azimuth DOA have shown that by incorporating a head-like scatter between the two antennas, not only high frequency ambiguity associated with phase wrapping is eliminated, but also the DOA sensitivity is improved significantly. By applying genetic algorithm, the scatter is optimized in terms of geometry and material parameters to satisfy that the response function is incident angle dependent for all directions in 3-D. Simulated 3-D DOA estimation errors of the optimized monopole/scatterer configuration show an encouraging accuracy and sensitivity. However, the large DOA estimation error near $\phi=0°$ and $180°$ and $\theta=0°$ should be further studied and eliminated. One possible solution may be applying scatterer optimization of both geometry and material parameters such as ε, μ, $\tan\delta$. Using other practical antennas with higher directivity instead of monopoles may also help.

REFERENCES

[1] S. E. Lipsky, Microwave Passive Direction Finding, John Wiley & Sons, Inc., New York, 1987.

[2] L.C. Godara, "Application of antenna arrays to mobile communications. II. Beam-forming and direction-of-arrival considerations," Proc. IEEE, Vol. 85, no. 8, pp. 1195-1245, 1997.

[3] B. C. J. Moore, Introduction to the Psychology of Hearing, University Park Press, Baltimore, Maryland, 1977, pp. 169-208.

[4] E. Villchur, Acoustics for Audiologists, Singular Publishing Group, 2000.

[5] W. A. Yost, Fundamentals of Hearing: An Introduction, 4th ed., Academic Press, 2000.

[6] S. S. Stevens, and E. B. Newman, "The Localization of Actual Sources of Sound," Am. J. Psychol., Vol. 48, no. 2, pp. 297-306, 1936.

[7] T. T. Sandel, D. C. Teas, W. E. Feddersen, and L. A. Jeffress, "Localization of sound from single and paired sources," J. Acous. Soc. Am., vol. 27, issue: 9, pp. 842-852, 1955.

[8] L. A. Jeffress, "Detection and Lateralization of Binaural Signalsl," Audiology, 10, pp. 77-84, 1971.

[9] H. Xin and J. Ding, "An improved two-antenna direction of arrival (DOA) technique inspired by human ears," IEEE AP-S Intl Symp. Dig., pp. 1-4, July. 2008.

[10] R. Zhou, H. Zhang and H. Xin, "Improved Two-Antenna Direction Finding Inspired by Human Ears," IEEE Trans. Antennas Propag., July. 2011.

[11] R. O. Schmid, "Multiple emitter location and signal parameter estimation," IEEE Trans. Antennas Propagat., vol. 34, pp. 276-280, 1986.

[12] David Edward Goldberg, Genetic algorithms in search, optimization, and machine learning, Addison-Wesley Pub., 1989.